Materials Science & Engineering A 651 (2016) 548–555

Contents lists available at ScienceDirect

Materials Science & Engineering A

journal homepage: www.elsevier.com/locate/msea

Nanoindentation investigation on the creep mechanism in metallic glassy films

Y. Ma [a], G.J. Peng [a], Y.H. Feng [b], T.H. Zhang [a,*]

[a] College of Mechanical Engineering, Zhejiang University of Technology, Hangzhou 310014, China
[b] State Key Laboratory of Nonlinear Mechanics (LNM), Institute of Mechanics, Chinese Academy of Sciences, Beijing 100190, China

ARTICLE INFO

Article history:
Received 26 May 2015
Received in revised form
5 November 2015
Accepted 6 November 2015
Available online 10 November 2015

Keywords:
Metallic glass
Nanoindentation
Creep
Free volume
Shear transformation zone

ABSTRACT

Using the magnetron sputtering technique, two metallic glassy films namely $Cu_{44.3}Zr_{45.1}Al_{10.6}$ and $Cu_{44.2}Zr_{43}Al_{11.3}Ti_{1.5}$ were prepared by alloy targets. The minor Ti addition effectively induces excess free volume. Upon spherical nanoindentation, the creep behaviors of both films were studied at various peak loads. As the increase of peak load, the creep deformations became more severely in both samples. Interestingly, Cu–Zr–Al–Ti film crept stronger than Cu–Zr–Al at small-load holdings (nominal elastic regimes), whereas it is opposite at high-load holdings (plastic regimes). The creep characteristic could be intrinsically related to the scale variation of the shear transformation zone (STZ) with Ti addition. Statistical analysis was employed to estimate the STZ volume, which increased by 60% with Ti addition in the Cu–Zr–Al film. The finite element modeling indicated that STZs would be activated even at the minimum load we adopted. Higher activation energy of larger STZs in Cu–Zr–Al–Ti enables less flow units, which offsets the creep enhancement by the excess free volume with Ti addition. The deeper the pressed depth of the indenter, the more contribution of the STZ operation on creep deformation. In addition, experimental observation on the creep flow rates implies that STZ could be the dominating mechanism at the steady-state creep. This study reveals that STZ volume could also be important to the time-dependent plastic deformation in metallic glass, besides as a key parameter for instantaneous plasticity.

1. Introduction

For the last several decades, the mechanism of plastic deformation in metallic glasses has been widely investigated [1,2]. This is due to both fundamental and technological importance of these materials in the condensed mater research. Having clear difference in atomic structure from its crystalline counterparts, shear transformation zones (STZs) are usually considered playing a vital role to in allowing irreversible deformation in metallic glasses [3]. The activation and evolution of STZs are pivotal to the shear banding events as well as the instantaneous mechanical response [4,5]. In recent years, following the cooperative shear model (CSM) by Johnson and Samwer [6], Pan et al. estimated the STZ volume experimentally (using rate-jump method) and found a correlation between STZ volume and plasticity of metallic glasses [7,8]. Additionally, free volume is another important atomic-level feature which can intrinsically control plasticity [9–11]. By adding just 2% Ti, plasticity of a Cu–Zr–Al metallic glass can be greatly enhanced due to the induced excess free volume [12]. The creation and annihilation of free volume could sustain the homogeneous creep flow at high temperature [13] or/and nanoscale [14].

Based on nanoindentation, creep behaviors of metallic glasses can be studied at small region, ignoring the limit of required standard size in traditional creep testing. In addition, the holding stage could be time-saving due to the high accuracy for obtaining the time-dependent plastic deformation. However, the stress distribution beneath the indenter is much more complicated and plastic deformation always occurred before the holding stage [15–18]. Thus, metallic glasses having high glass transition temperature (T_g) can even creep at room temperature in nanoindentation. To authors' best knowledge, the creep behaviors of metallic glasses concerned with loading rate [16], holding load [16,17] and initial strain [18] were qualitatively explained through free volume. In our previous work, the loading rate effect on creep was found to be composition-dependent and apparently related to the STZ size [19]. Though the exact creep response on the variation of STZ size is far from understanding due to the changes of other structural or physical parameters at the same time as the composition changes. With this in mind, creep behaviors of Cu–Zr–Al and Cu–Zr–Al–Ti

* Corresponding author.
E-mail address: zhangth@zjut.edu.cn (T.H. Zhang).

http://dx.doi.org/10.1016/j.msea.2015.11.014
0921-5093/

metallic glassy films were investigated in the present work. The minor Ti addition was confirmed to effectively increase free volume content while not changing the intrinsic parameters such as Poisson's ratio or elastic modulus [12]. The STZ volumes of both films were carefully estimated in nanoindentation based on a popular statistical method. Here, we aim to study the effect of Ti addition on creep deformation for further revealing the creep mechanism in metallic glasses.

2. Experimental procedures

The Cu–Zr–Al and Cu–Zr–Al–Ti thin films were deposited on clean silicon wafer in a DC magnetron sputtering system (Kurt J. Lesker PVD75) at room temperature in pure argon gas. The 2-in. alloy targets adopt in the chamber were $Cu_{45}Zr_{48}Al_7$ and $Cu_{45}Zr_{46}Al_7Ti_2$, respectively. The target is installed at the bottom while the silicon wafer is stick on the sample platform, which is right above the target. The target-to-substrate distance is kept constant, which is equal to 100 mm. The base pressure of the chamber was kept about $5^{*}10^{-7}$ Torr before deposition and working argon pressure was set at about 1 mTorr. The power on the target was fixed at 180 W during the deposition and the sputtering time was for 1 h. The structures of both films were detected by X-ray diffraction (XRD, PANalytical X'Pert PRO) with Cu K_α radiation. The thicknesses of the as-deposited films were measured from cross-sections by scanning electron microscope (SEM, MOI-ZEISS). By means of X-ray energy dispersive spectrometer (EDS) attached on the SEM, the chemical compositions of both films can be accurately detected. The thermal properties of the samples (peeled from the substrate) were estimated using the differential scanning calorimetry (DSC, NETZSCH) with heating rate of 20 K/min.

The nanoindentation experiments were conducted at constant temperature of 20 °C on Agilent Nano Indenter G200 with a spherical indenter, with an effective radius of 3.15 μm upon calibrating on standard fused silica. The displacement and load resolutions of the machine are 0.01 nm and 50 nN, respectively. The as-deposited films could be directly applied on nanoindentation testing due to the ultralow roughness of metallic glassy film surface [19]. For the creep tests, a constant-load holding method was used, and the displacement of indenter into the surface at a prescribed load could be continuously recorded. The indenter was held for 500 s at maximum loads of 1 mN, 2 mN, 4 mN, 8 mN, 12 mN and 16 mN in both samples. The loading rate was a constant value, which was equal to 0.5 mN/s. The reliability of the creep results was confirmed by conducting ten independent measurements. The STZ volume was estimated by a statistical measurement, in which 64 loading tests were conducted on each sample. The loading rate and the maximum load were 0.5 mN/s and 15 mN, respectively. All the nanoindentation tests were carried out until thermal drift reduced to below 0.02 nm/s. Furthermore, drift correction which was calibrated at 10% of the maximum load during the unloading process would be strictly performed.

3. Results and discussion

The chemical compositions of the as-deposited films were $Cu_{44.3}Zr_{45.1}Al_{10.6}$ and $Cu_{44.2}Zr_{43}Al_{11.3}Ti_{1.5}$, which were much close to the target alloys. Each elements were uniformly distributed as shown in the layer probes in Supplementary material. Fig. 1 (a) shows the typical X-ray diffraction patterns of the as-prepared Cu–Zr–Al and Cu–Zr–Al–Ti films. It is clear that only a broad diffraction peak can be detected in each sample, which represents a

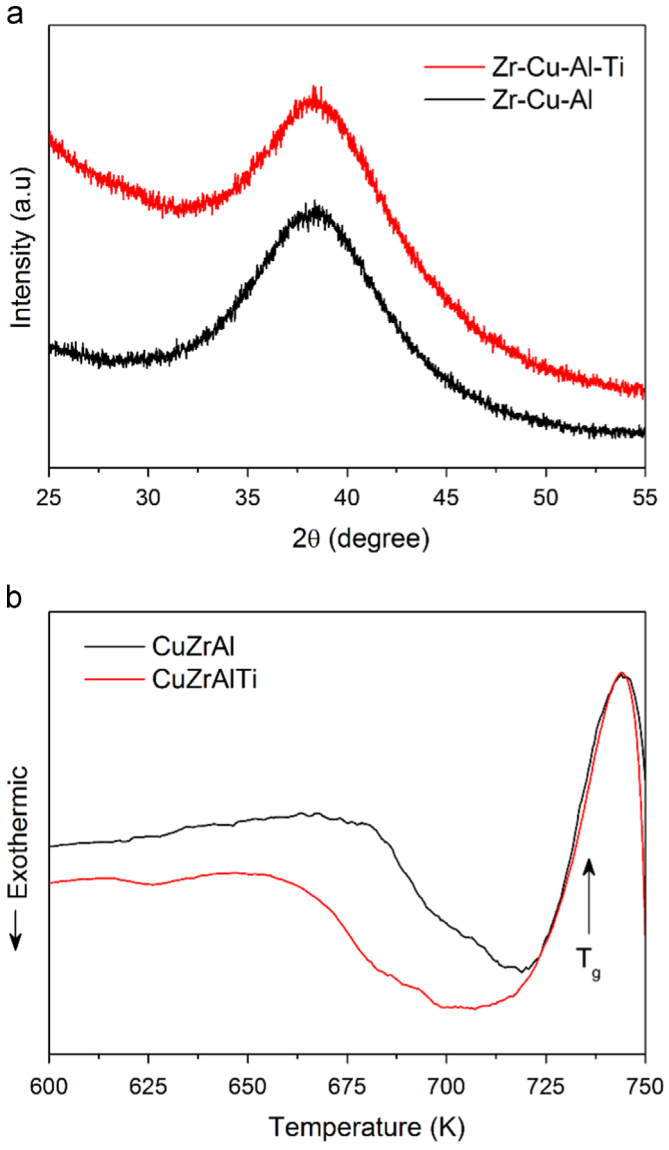

Fig. 1. (a) Typical XRD patterns and (b) the details of the sub-T_g regions for the DSC traces of the Cu–Zr–Al and Cu–Zr–Al–Ti films.

crystal-free structure. Fig. 1(b) shows an enlargement of the sub-T_g region for the DSC curves, which corresponds to the enthalpy released during structure relaxation and can be strongly linked with the free volume content. It clearly shows the structure relaxation process occurred more pronounced in the Cu–Zr–Al–Ti compared with the Cu–Zr–Al, confirming the effect of Ti addition on inducing large amount of free volume. Meanwhile, the glass transition temperature T_g of the films can be obviously observed at about 735 K, as the arrow indicates.

With cleavage cracking of the Si substrate by a diamond knife, a rapid tensile fracture occurs in the film. The thicknesses of Cu–Zr–Al and Cu–Zr–Al–Ti films can be directly measured to be about 1.60 μm and 1.48 μm, from cross-sections in Fig. 2. The thickness discrepancy between the two films could be largely induced by the external configurations, such as the thickness of target alloy, the intensity of magnetic core or the target-to-sample orientation. For the shear-dominated fracture in metallic glass, the final fracture surface usually consists of a smooth region caused by slid shear and a vein pattern region caused by subsequent crack. As shown in Fig. 2(a), a smooth region with width of 500–1000 nm and vein pattern with about 500 nm diameter can be observed in Cu–Zr–Al

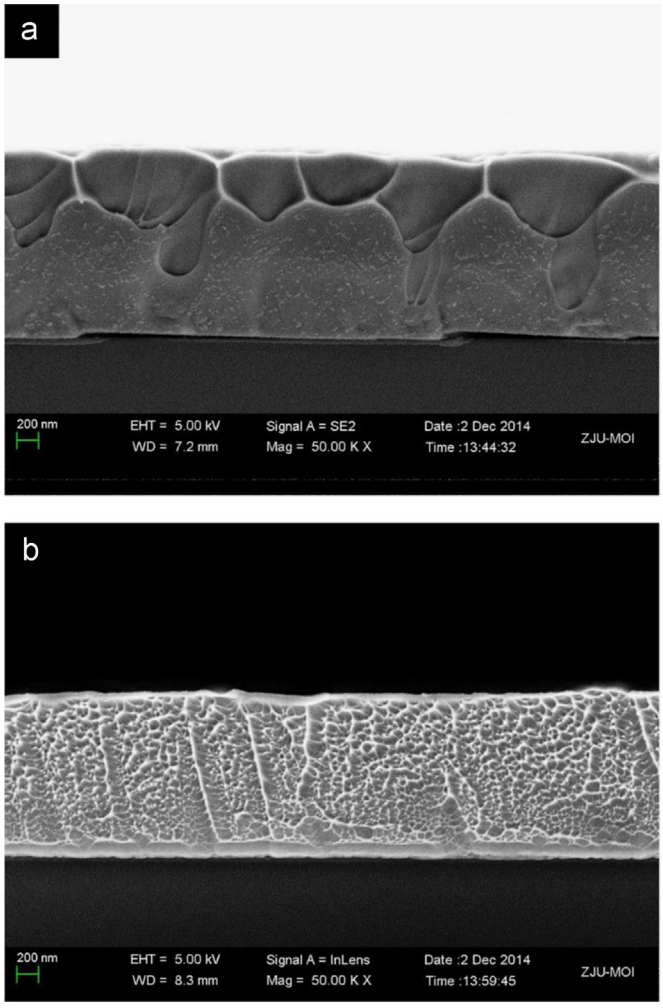

Fig. 2. Typical cross-sections of the Cu–Zr–Al and Cu–Zr–Al–Ti films by SEM.

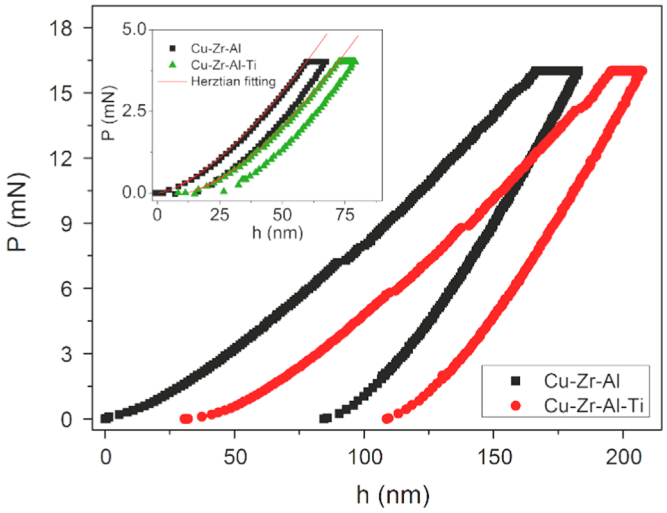

Fig. 3. Representative load–displacement (P–h) curves of the 500 s-holding creep tests with maximum loads of 16 mN and 4 mN (inset) in Cu–Zr–Al and Cu–Zr–Al–Ti films. Displacements of the Cu–Zr–Al–Ti film have been offset for clearly viewing.

film. In comparison, the characteristics of fracture surface morphology in Cu–Zr–Al–Ti film were apparently below 200 nm, as shown in Fig. 2(b). In the bulk sample, Ti addition on Cu–Zr–Al metallic glass effectively increased the density of shear bands during plastic deformation [12]. Here, the same effect of Ti addition would be concluded indirectly from the smaller-sized vein-pattern fracture morphology. The SEM observations implies an enhanced ductility in Cu–Zr–Al film with Ti addition [20], which was consistent with Chen's [12]. What is more, the thinner smooth region indicates a relatively weaker resistance to the plastic shearing in Cu–Zr–Al–Ti film.

Fig. 3 exhibits the typical creep P–h curves at 16 mN and 4 mN (in the inset) for both films as illustration. By applying 16 mN, the indenter was certainly pressed into plastic region for the both films that pop-ins can be directly observed. And the initial strain before holding stage could be estimated as about 5.2% (ε_i=0.2($\frac{\alpha}{R}$) α is the contact radius, R is the tip radius), far beyond the general elastic limit for metallic glasses. For the 4 mN-holding tests, the loading sequences of both films were totally overlapped with Hertzian elastic fitting lines [21], given by:

$$P = \frac{4}{3} E_r \sqrt{R} h^{1.5} \quad (1)$$

where E_r is the reduced elastic modulus which accounts for that the elastic displacement occurred in both the tip and sample. This apparently implies the 4 mN loading sequence could be elastic, though the applied strain has reached 2.7%. Clearly, the time-dependent plastic deformation occurred in both cases for the two films. It should be noted that the maximum indentation depths even in 16 mN tests are about 10% of the film thickness. Therefore the substrate influence is negligible here.

Fig. 4 shows the corresponding creep curves during the holding stages, in which creep displacements were plotted with the holding time. Two distinct stages can be divided for the creep curves as transient creep and steady-state creep. At the transient stage, the displacement increases relatively fast but the creep rate drops rapidly. Then the creep displacement turns to be slowly and almost linearly increased with time at the steady-state stage. For authenticity, creep curve for each case were averaged from 5 to 8 effective independent indentations. For both films, the creep deformations were more severely at higher loads, i.e. larger initial strain at the onset of holding stage in the spherical indentation. This can be qualitatively explained by the excess free volume generated and more STZs activated in the more severely plastic regime [18]. Furthermore, the peak load (or initial strain) enhancement on creep was found to be weakened in the sample with minor Ti addition.

Fig. 5(a) summarizes the total creep displacements during the 500 s holding at various peak loads for the two films. It is clear that the creep deformation was more obviously occurred in Cu–Zr–Al–Ti in comparison to Cu–Zr–Al at the peak loads of 1 mN and 2 mN. As the increase of peak load, the creep displacements of both samples reached almost the same about 8.5 nm at 4mN holding and then turned to be more pronounced in Cu–Zr–Al film at 8 mN, 12 mN and 16 mN. The flow rate of steady-state creep (defined as the last 200 s holding here) can more intrinsically reflect the creep resistance of material under certain conditions. By linear fitting, the flow rate of each creep curve was obtained for both samples as shown in Fig. 5(b). In this scenario, the displacement of steady-state creep was slower increased with time in Cu–Zr–Al–Ti than that in Cu–Zr–Al for all the cases. The distinction of flow rates between Cu–Zr–Al–Ti and Cu–Zr–Al films at higher loads can be more clearly observed in the inset, in which the data was linearly plotted. The present results are apparently contradictory to Yoo's that the more free volume content the sample contained, the easier the occurrence of creep in metallic glass [18]. Actually, it's widely believed that free volume facilitates creep flow and annealing has been confirmed as an effective treatment to strengthen the creep resistance in metallic glass [15]. Here, the Cu–Zr–Al–Ti film with more free volume exhibited a generally

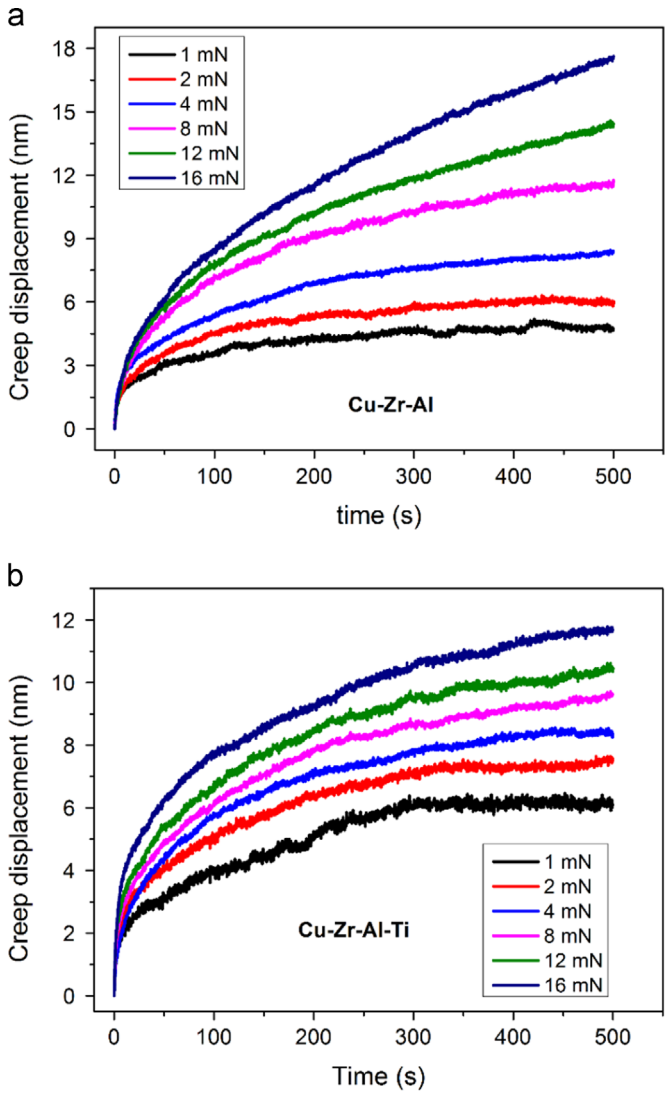

Fig. 4. Indentation creep displacements versus holding time for various peak loads in the (a) Cu–Zr–Al and (b) Cu–Zr–Al–Ti films.

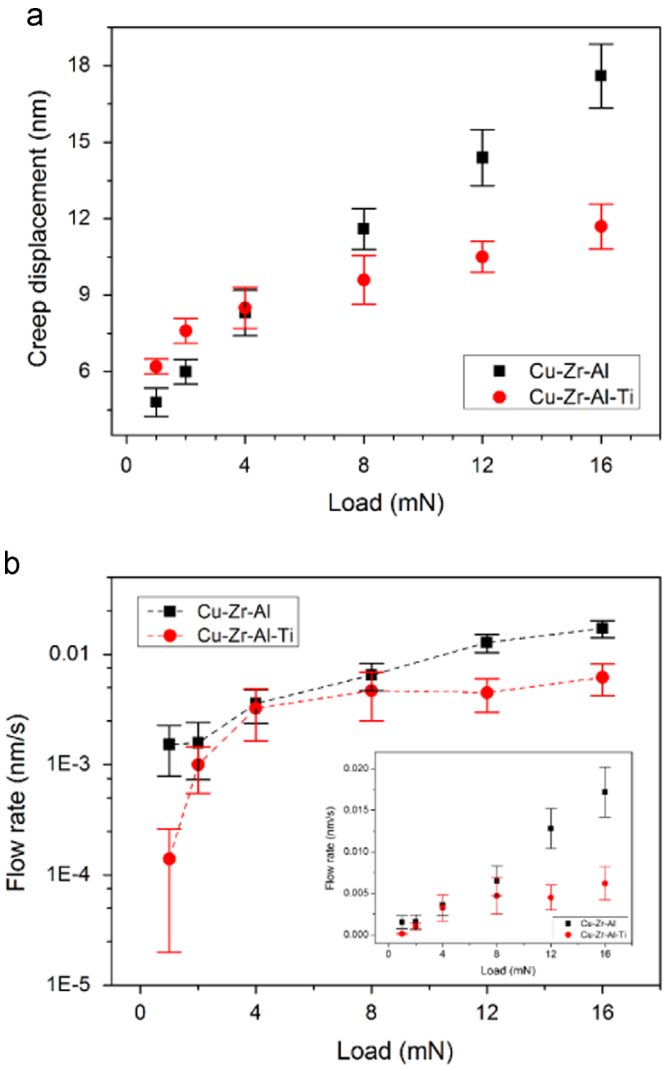

Fig. 5. (a) Creep displacements of both films as a function of peak load. (b) Flow rates of the steady-state creeps for both films as a function of peak load.

weakened creep flow at the high-load holdings compared to the Cu–Zr–Al film. The present work implies that the free volume might not be the only determinative structure characteristic on the creep flow in metallic glasses. From the scientific points of view, the deformation mechanism of the dynamic flow process during the creep in nanoindentation has not been discussed well.

In crystalline alloys, the time-dependent plastic deformation in nanoindentation could be ascribed to various mechanisms such as dislocation glide (or climb), twins deformation, lattice diffusion and boundary diffusion et al. [22]. For metallic glasses, the free volume evolution [14] and interfacial diffusion [23] were expected to be the deformation modes of creep flow within elastic and/or shallow depth regime. In present study, the cases with peak loads of 1 mN, 2 mN and 4 mN could meet the requirement of free volume-dominating creep. Meanwhile, the initial pressed depth of 8 mN holding had reached about 100 nm, which is far beyond the critical penetration depth for interfacial diffusion as Wang et al. reported [23]. Therefore, free volume creation and annihilation would not be the main deformation mechanism for the 8 mN, 12 mN and 16 mN creep tests, and interfacial diffusion could be insignificant. Conceivably, the STZs would be activated and sustained the creep deformation in the plastic regime. This does not deny the importance of free volume, which could not only increase the atom mobility but also provide fertile regions for the STZ activation. Here we emphasize the dynamic process of creep flow upon STZs. The instantaneous plasticity of metallic glasses was reported to be closely tied with the STZ volume [7]. Now one pertinent question arises very naturally: Do there exist any correction between time-dependent plastic deformation and STZ volume? Aiming to answer this very question, the STZ volumes of two films need to be calculated first.

Fig. 6(a) and (b) shows the typical *P–h* curves of Cu–Zr–Al and Cu–Zr–Al–Ti films at maximum load 15 mN with 1 s holding. The pop-in events with scale of 1–2 nm can be observed in each sample. The initial loading curve can also be completely fitted by the Hertzian elastic contact theory, according to Eq. (1). It should be mentioned that the Hertzian fitting line exactly deviates from the *P–h* curve at the position of first pop-in in both samples. This clearly indicates the transition from elastic to elastic–plastic once the first pop-in emerges, which also could be regarded as the onset of yielding in the present samples [24]. Fig. 6(c) shows the load range of first pop-in in all the 64 nanoindentations for the two films. The valid critical load is roughly within 5–10 mN for Cu–Zr–Al and 4.5–7 mN for Cu–Zr–Al–Ti. Fig. 7(a) shows correlation between the critical load and displacement at first pop-in position for Cu–Zr–Al and Cu–Zr–Al–Ti and the power-law fitting expressions are $P=0.00802h^{1.5}$ and $P=0.00796h^{1.5}$, respectively. The

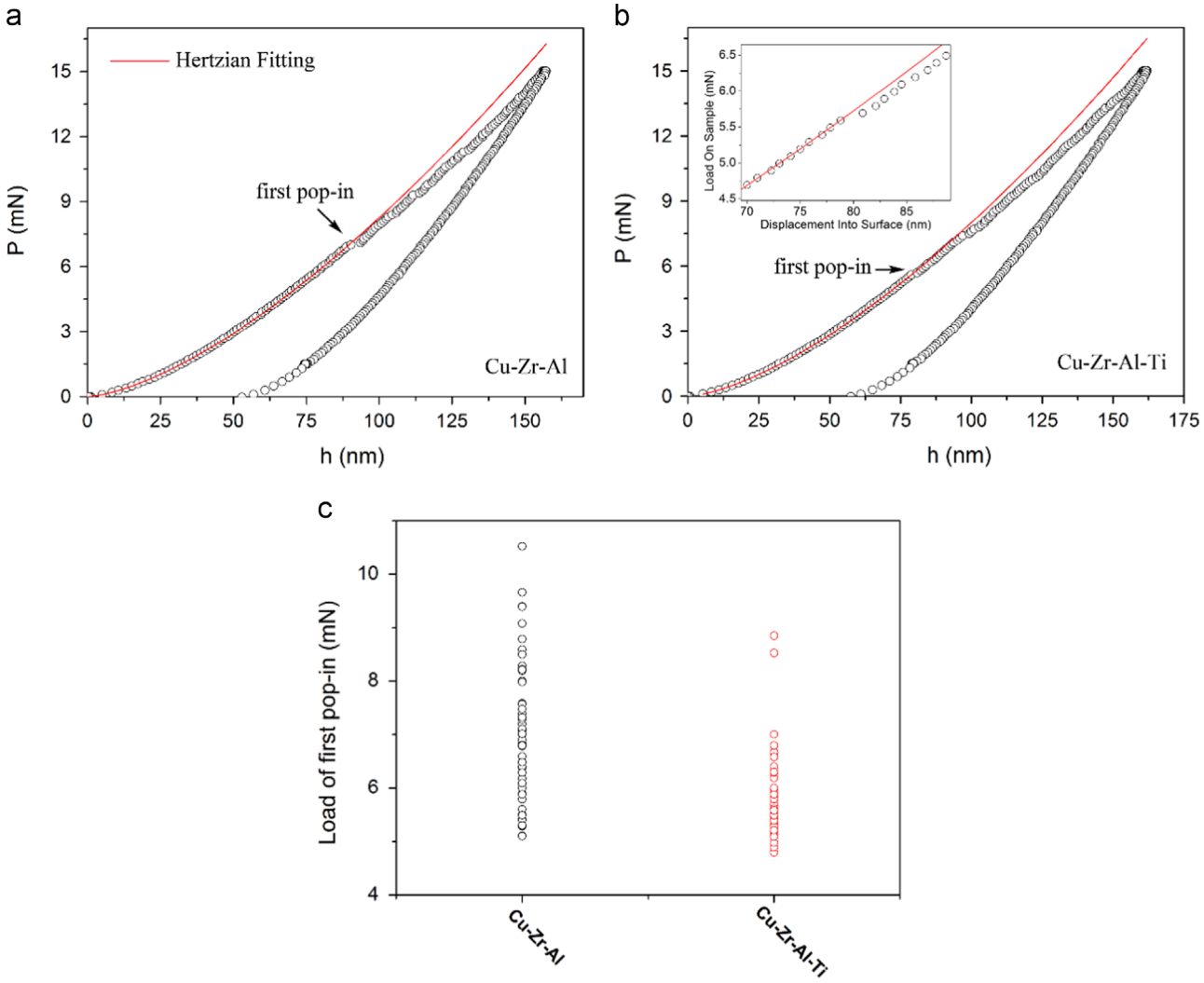

Fig. 6. Typical 15 mN *P–h* curves of (a) Cu–Zr–Al and (b) Cu–Zr–Al–Ti films, pop-in can be detected in each sample; (c) The load range of first pop-in in all the 64 nanoindentations for the two films.

elastic modulus can thus be calculated as 108.3 GPa and 107.5 GPa for Cu–Zr–Al and Cu–Zr–Al–Ti films. According to Bei's theory, the maximum shear stress τ_m underneath the indenter when the first pop-in event occurs represents the shear strength for the onset of plasticity [24]. For a spherical indenter, the τ_m happens at about half the elastic contact radius $a = \sqrt{Rh_e}$ right below the contact surface, given by:

$$\tau_m = 0.445P_m \tag{2}$$

where P_m is the mean pressure given by:

$$P_m = \frac{P}{\pi a^2} \tag{3}$$

P and h_e are the load and displacement at first pop-in. The P_m values obtained from the 64 *P–h* curves for the both films were plotted with the measurement numbers in Fig. 7(b). It is clear that the P_m of the Cu–Zr–Al–Ti was apparently smaller in value and less diversified than that of the Cu–Zr–Al. The mean values of P_m were 8.12 GPa and 7.58 GPa for Cu–Zr–Al and Cu–Zr–Al–Ti films, respectively. Accordingly, the τ_m of both samples can be obtained and plotted as the cumulative distribution in Fig. 7(c). The experimental results agree well with Bei's theory that the upper limit of the valid τ_m were 4.04 GPa and 3.74 GPa for the Cu–Zr–Al and Cu–Zr–Al–Ti, respectively, which closely approach the theoretical shear strengths 4 GPa and 3.95 GPa (estimated by $G/10$ [25], G is the shear modulus and can be estimated as $E/2(1+\nu)$, here ν is 0.36 for both samples). Based on Schuh's work [26], the activation volume of the nucleation events for the onset of the plasticity can be estimated through the statistical method, which relies on the cumulative distribution of the yield strength. Recently, Jang et al. developed and applied such statistical method on metallic glass to estimate the STZ activation volume [27]. The cumulative probability of the thermally-assisted and stress-biased τ_m can be described as the red fitting lines in Fig. 7(c), given by:

$$f = 1 - \exp\left[-\frac{kT\dot{\gamma}_0}{V^*(d\tau/dt)}\exp\left(-\frac{\Delta F^*}{kT}\right)\exp\left(\frac{\tau V^*}{kT}\right)\right] \tag{4}$$

where k is the Boltzmann constant, T is the temperature, $\dot{\gamma}_0$ is the attempt frequency, and ΔF^* is the Helmholtz activation energy, the ratio of $d\tau/dt$ is a constant in the fixed loading rate-control mode. V^* is the activation volume, can be calculated from the slop of $\ln[\ln(1-f)^{-1}]$ vs. τ_m by converting the Eq. (4) to be as:

$$\ln\left[\ln(1-f)^{-1}\right] = \left\{\frac{\Delta F^*}{kT} + \ln\left[\frac{kT}{V^*(d\tau/dt)}\right]\right\} + \frac{\tau V^*}{kT} \tag{5}$$

Fig. 7(d) shows the correlation between $\ln[\ln(1-f)^{-1}]$ and τ_m for both samples, in which the value of f lies between 0.2 and 0.8 was adopted. And then the converted curves were fitted linearly to

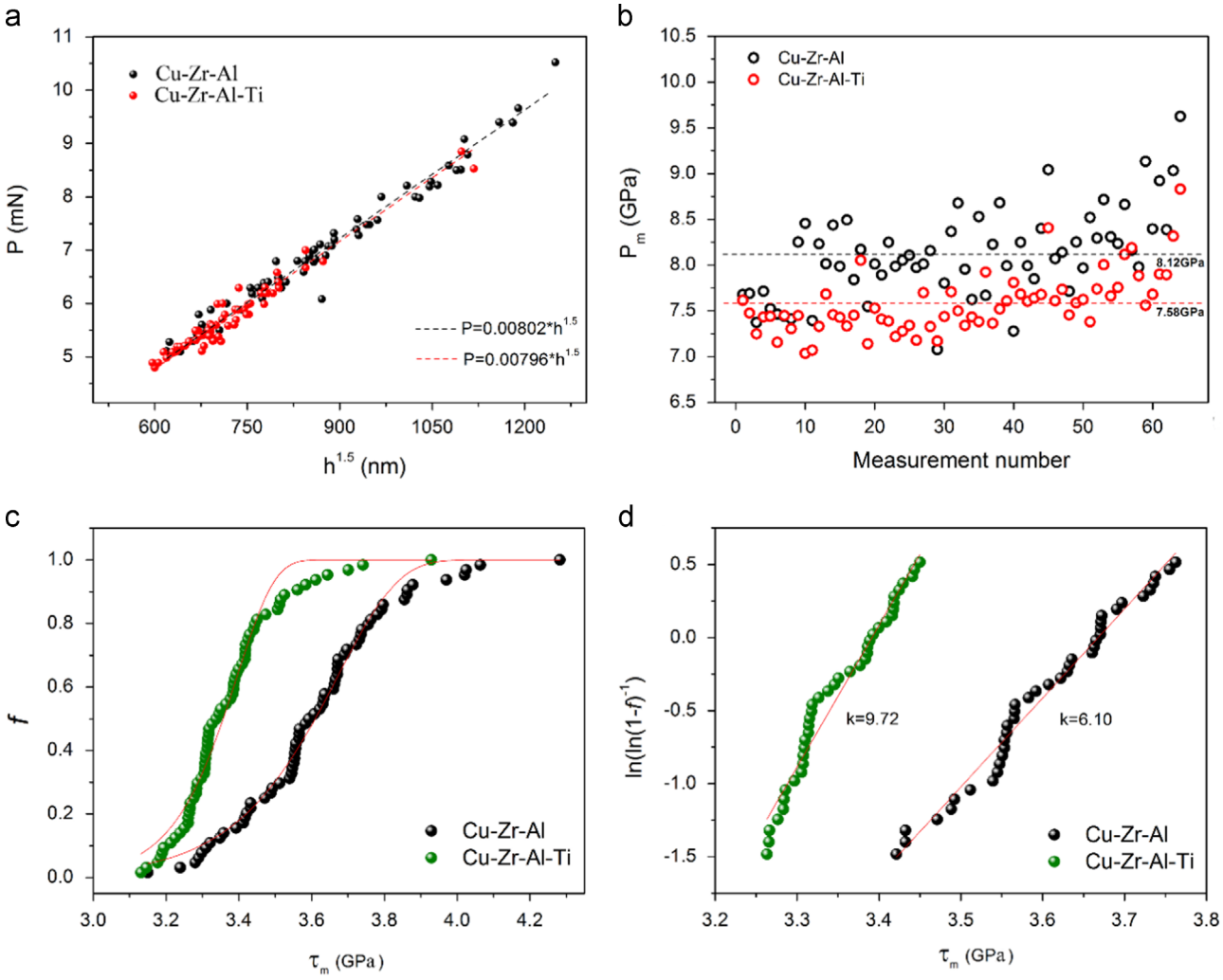

Fig. 7. (a) Statistics of 64 P–$h^{1.5}$ pairs at the first pop-in position of both films; (b) The values of mean pressure P_m for both films, plotted with the measurement number. (c) Cumulative probability distribution of the maximum shear stress τ_m at first pop-in; (d) the value of $\ln(\ln(1-f)^{-1})$ versus maximum shear stress τ_m, linear fitting is employed to estimate the activation volume. (For interpretation of the references to color in this figure legend, the reader is referred to the web version of this article.)

obtain the slopes, 6.10 for Cu–Zr–Al and 9.72 for Cu–Zr–Al–Ti. Once the V^* is determined, the STZ volume Ω can be accordingly estimated by the cooperative shear model (CSM) of Johnson and Samwer [6], given by:

$$\Omega = \frac{\tau_0}{6R_0G_0\gamma_C^2\xi(1-\tau/\tau_0)^{1/2}}V^* \tag{6}$$

where $R_0 \approx 1/4$ and $\xi \approx 3$ are constants, τ and τ_0 are threshold shear resistances at temperature T and 0 K, G_0 is the shear modulus at 0 K, the average elastic limit $\gamma_C \approx 0.027$, $\tau_0/G = 0.036$, the value of τ/τ_0 can be estimated from the constitutive equation

$$\tau/G = \gamma_{C0} - \gamma_{C1}(T/T_g)^{2/3} \tag{7}$$

where $\gamma_{C0} = 0.036 \pm 0.002$, $\gamma_{C1} = 0.016 \pm 0.002$, shear modulus G has a weak temperature dependency for a metallic glass and would not affect the calculation according to the dense-packing hard-sphere model of metallic glass [28]. The glass transition temperature in the Cu–Zr–Al film was detected as 735 K and would not be altered with Ti addition in Fig. 1(b). Computed results of V^* and Ω using the statistical method are summarized in Table1. The STZ volumes of the both samples are consistent with those reported by experimental calculation and simulation prediction [13,29,30]. 60% enlargement on the STZ volume, from 0.552 nm^3 to 0.884 nm^3 with 1.5% Ti addition, could explain the significant improvement of ductility in the bulk one in turn [7,12]. Large STZs can produce large internal concentrations which facilitate activation of surrounding STZs, promoting multiple shear bands. The effect of Ti addition on STZ volume could be reasonable due to the increased large amount of free volume. Pan et al. also reported less dense atomic packing has larger STZ volume in a Zr–Cu–Ni–Al metallic glass [8]. However, it does not reach an agreement on the correlation between the free volume content and STZ volume that Jang et al. reported a negative effect of free volume on STZ volume [27].

Table1
Summary of elastic modulus, maximum shear stress, STZ activation volume and STZ volume in Cu–Zr–Al and Cu–Zr–Al–Ti films determined by statistical method.

Composition	E (GPa)	Mean τ_m (GPa)	V^* (nm^3)	Ω (nm^3)
Cu–Zr–Al	108.3	3.37	0.025	0.552
Cu–Zr–Al–Ti	107.5	3.61	0.04	0.884

STZ is thought to be the plastic unit in metallic glass. In the light of STZ evolution, the creep displacement at various loads in Fig. 5(a) could be explained qualitatively. Larger STZs require higher activation energy (or stress), enabling less amount of the flow unit to be driven in the Cu–Zr–Al–Ti film during the holding stage in plastic regime. For spherical tip, the indentation process

can be divided into three ordinal phases: elastic deformation, elastic–plastic deformation and fully plastic deformation. In consideration of the large tip radius of 3.15 μm, the elastic zone is still considerable to the whole deformation even at 16 mN loading. When the maximum shear stress beneath the indenter exceeds the yield stress of material, the STZs would be activated and initiate shear banding. On account of this, the Cu–Zr–Al–Ti film would creep more easily in the elastic regime namely 1 mN, 2 mN and 4 mN holdings (free volume dominating). Then the more plastic deformation (provided numerous fertile sites for STZ activation) at the onset of holding, the more STZs would be operated to afford the creep flow cooperatively with free volume. It is conceivable that the Cu–Zr–Al–Ti film with larger-sized STZs showed a weak and slower increased creep deformation with the peak load than the Cu–Zr–Al film in plastic regimes namely 8 mN, 12 mN and 16 mN holdings. However, such explanation could not meet the experimental result well. Obviously, the almost same creep displacement at 4 mN for both films (Fig. 5(a)) and the always lower creep flow rates in Cu–Zr–Al–Ti film (Fig. 5(b)) are out of the scope of creep kinetics we expected. In Yoo's work [18], the creep displacements were almost the same in Cu–Zr samples with different components during elastic holding. The possible reason is that denser sample could generate more free volume during elastic deformation [31], enlarging free volume content at the onset of creep. While this reason could not be adopted here, for lacking concrete confirmation from computational simulation in Cu–Zr–Al with minor Ti addition.

Though the Hertzian elastic fitting is originally used in the pure elastic loading, it does not mean the material at 4 mN suffered pure elastic stress in turn (even if 4 mN loading curve was perfectly fitted). Fig. 8 shows the shear stress distribution within Cu–Zr–Al film under small loads by finite element modeling (FEM), of which details were also illustrated in Supplementary material. Fig. 8(a) indicates the purely elastic deformation could only occur before the displacement of 22 nm (0.9 mN) (such critical displacement was a little smaller in Cu–Zr–Al–Ti). Fig. 8(b) shows the maximum shear stress beneath 1 mN holding had reached the theoretical yield strength which was defined at the first pop-in position aforementioned. And the region suffered yielding gradually enlarges as the applied load increases to 2 mN and 4 mN, as shown in Fig. 8(c) and (d). The Cu–Zr–Al–Ti film exhibited similar results (not shown here). That is to say, the indenter had actually penetrated into the elastic–plastic region at 1 mN, 2 mN and 4 mN, while it's too weak to be discernable in the loading sequence. Thus the STZs would be activated during these small-load holdings, at least within the regions suffered yield stress. Due to the stress gradient, the activated STZs might be unable to reach the critical collection for the formation of a shear band nucleus (i.e, pop-in

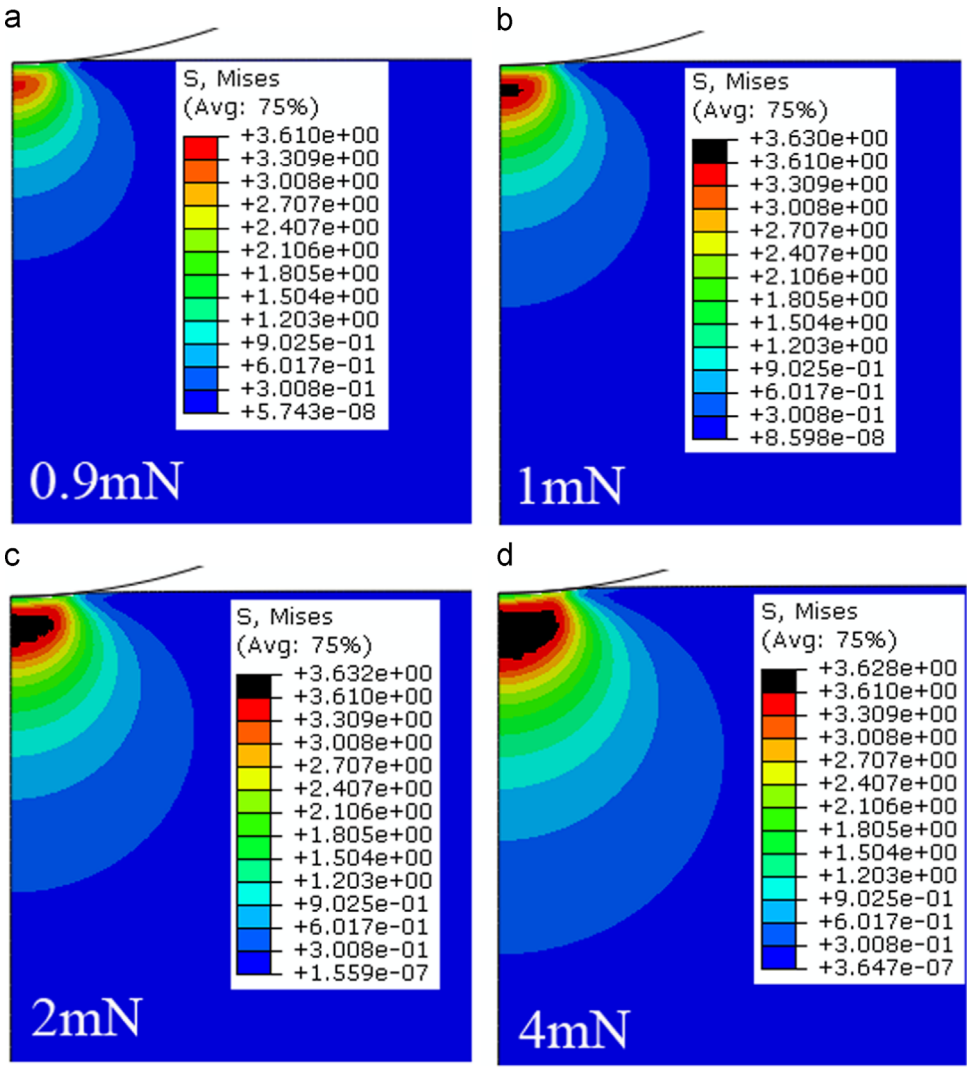

Fig. 8. Stress distribution beneath the indenter in the Cu–Zr–Al film by finite element modeling for (a) 0.9 mN; (b) 1 mN; (c) 2 mN; (d) 4 mN. The black region represents the mean yield stress.

events). In light of this, the 1 mN, 2 mN and 4 mN creeps would deform upon creation and annihilation of free volume combined with operation of the partially activated STZs. For the 4 mN holding, the STZs would play an important role on creep deformation. The smaller-sized STZs in Cu–Zr–Al could compensate the deficiency in free volume and accordingly promote the creep mobility. Furthermore, the slower creep flow at steady stage of Cu–Zr–Al–Ti (Fig. 5(b)) implies that free volume mainly works at the transient creep and STZs are decisive to the steady-state flow of metallic glass.

It should be reiterated that, this study is not conflict with the previous reports that free volume could promote the creep flow. The STZ volume might be little changed or even decreased, which was leave out of consideration in those studies [15,17,18]. Indentation creep would depend on multiple intrinsic and/or external parameters in metallic glasses. The present study intends to describe the time-dependent plastic deformation basically from the deformation unit combined with free volume. Still much more investigates need to be carried out to get insights into the creep characteristics among various kinds of metallic glasses.

4. Conclusion

The effect of 1.5% Ti addition on the room temperature creep behaviors in a Cu–Zr–Al metallic glassy film was investigated by employing the spherical nanoindentation. Free volume content can be clearly enlarged with the minor Ti addition in the sample. With Ti addition, the creep flow was enhanced in the nominal elastic regimes, whereas an apparently depression was observed at the plastic-holding creep. The STZ volume was estimated by statistical method, which increased from 0.552 nm^3 to 0.884 nm^3 with Ti addition in the film. The FEM results indicated that STZs would actually be activated even at 1 mN holding, though the collection to arise shear band was not sufficient. From the perspective of deformation unit, the creep characteristic with minor Ti addition in Cu–Zr–Al film can be explained. The current finding provides new insight into understanding the time-dependent plastic deformation of metallic glasses.

Acknowledgment

The support from the National Natural Science Foundation of China (Grant nos. 11025212, 11272318, 11402233, 11302231 and 11502235) and Zhejiang Provincial Natural Science Foundation of China (Grant no. LQ15A020004) are gratefully acknowledged.

Appendix A. Supplementary material

Supplementary data associated with this article can be found in the online version at http://dx.doi.org/10.1016/j.msea.2015.11.014.

Reference

[1] A.S. Argon, H.Y. Kuo, Mater. Sci. Eng. 39 (1979) 101–109.
[2] M.L. Falk, J.S. Langer, Phys. Rev. E 57 (1998) 7192–7205.
[3] A. Argon, Acta Metall. Mater. 27 (1979) 47–58.
[4] P.S. Steif, F. Spaepen, J.W. Hutchinson, Acta Metall. 30 (1982) 447–455.
[5] H. Kimura, T. Masumoto, Acta Metall. 31 (1983) 231–240.
[6] W. Johnson, K. Samwer, Phys. Rev. Lett. 95 (2005) 195501.
[7] D. Pan, A. Inoue, T. Sakurai, et al., Proc. Natl. Acad. Sci. USA 105 (2008) 14769–14772.
[8] D. Pan, Y. Yokoyama, T. Fujita, et al., Appl. Phys. Lett. 95 (2009) 141909.
[9] T.W. Wu, F. Spaepen, Philos. Mag. B 61 (1990) 739–750.
[10] C.A. Schuh, T.C. Hufnagel, U. Ramamurty, Acta Mater. 55 (2007) 4067–4109.
[11] M. Stolpe, J.J. Kruzic, R. Busch, Acta Mater. 64 (2014) 231–240.
[12] L.Y. Chen, Z.D. Fu, G.Q. Zhang, et al., Phys. Rev. Lett. 100 (2008) 075501.
[13] M. Heggen, F. Spaepen, M.J. Feuerbacher, Appl. Phys. 97 (2005) 033506.
[14] B.G. Yoo, J.H. Oh, Y.J. Kim, et al., Int. J. Plast. 37 (2012) 108–118.
[15] B.G. Yoo, J.H. Oh, Y.J. Kim, et al., Intermetallics 18 (2010) 1898–1901.
[16] Y. Huang, J. Shen, Y. Chiu, J. Chen, J. Sun, Intermetallics 17 (2009) 190–194.
[17] B.G. Yoo, I.C. Choi, Y.J. Kim, et al., Mater. Sci. Eng. A 577 (2013) 101–104.
[18] B.G. Yoo, K.S. Kim, J.H. Oh, et al., Scr. Mater. 63 (2010) 1205–1208.
[19] Y. Ma, J.H. Ye, G.J. Peng, et al., Mater. Sci. Eng. A 622 (2015) 76–81.
[20] H. Kimura, T. Masumoto, in: F.E. Lubrosky (Ed.), London, Butterworth, 1983.
[21] K.L. Johnson, Contact Mechanics, Cambridge University Press, UK, 1987.
[22] W.B. Li, J. Henshall, R. Hooper, Acta. Metall. Mater. 39 (1991) 3099–3110.
[23] F. Wang, J.M. Li, P. Huang, et al., Intermetallics 38 (2013) 156–160.
[24] H. Bei, Z.P. Lu, E.P. George, Phys. Rev. Lett. 93 (2004) 125504.
[25] G.E. Dieter, D. Bacon, Mechanical Metallurgy, McGraw-Hill, New York, 1986.
[26] C.A. Schuh, A.C. Lund, J. Mater. Res. 19 (2004) 2152–2158.
[27] I.C. Choi, Y. Zhao, Y.J. Kim, et al., Acta. Mater. 60 (2012) 6862–6868.
[28] J.D. Bernal, Nature 185 (1960) 68–70.
[29] M. Zink, K. Samwer, W.L. Johnson, et al., Phys. Rev. B 73 (2006) 172203.
[30] A.S. Argon, L.T. Shi, Acta Metall. 31 (1983) 499–508.
[31] K.W. Park, C.M. Lee, M. Wakeda, et al., Acta Mater. 56 (2008) 5440–5450.